Journal of Hazardous Materials 176 (2010) 444–450

Contents lists available at ScienceDirect

Journal of Hazardous Materials

journal homepage: www.elsevier.com/locate/jhazmat

Thermodynamic modeling of ferric phosphate precipitation for phosphorus removal and recovery from wastewater

Tao Zhang, Lili Ding, Hongqiang Ren*, Zhitao Guo, Jing Tan

State Key Laboratory of Pollution Control and Resource Reuse, School of the Environment, Nanjing University, Nanjing 210093, Jiangsu, PR China

ARTICLE INFO

Article history:
Received 16 July 2009
Received in revised form 9 November 2009
Accepted 9 November 2009
Available online 13 November 2009

Keywords:
PHREEQC program
Ferric phosphate ($FePO_4{\cdot}2H_2O$)
Thermodynamic modeling
Saturation-index (SI)

ABSTRACT

Phosphorus removal and recovery by ferric phosphate ($FePO_4{\cdot}2H_2O$) precipitation has been considered as an effective technology. In the present study, we examined chemical precipitation thermodynamic modeling of the PHREEQC program for phosphorus removal and recovery from wastewater. The objective of this research was to employ thermodynamic modeling to evaluate the effect of solution factors on $FePO_4{\cdot}2H_2O$ precipitation. In order to provide comparison, with the evaluation of thermodynamic modeling, the case study of phosphate removal from anaerobic supernatant was studied. The results indicated that the saturation-index (SI) of $FePO_4{\cdot}2H_2O$ followed a polynomial function of pH, and the solution pH influenced the ion activities of ferric iron salts and phosphate. The SI of $FePO_4{\cdot}2H_2O$ increased with a logarithmic function of Fe^{3+}:PO_4^{3-} molar ratio (Fe/P) and initial PO_4^{3-} concentration, respectively. Furthermore, the SI of $FePO_4{\cdot}2H_2O$ decreased with a logarithmic function of alkalinity and ionic strength, respectively. With an increase in temperature, the SI at pH 6.0 and 9.0 decreased with a linear function, and the SI at pH 4.0 followed a polynomial function. For the case study of phosphate removal from anaerobic supernatant, the phosphate removal trend at different pH and Fe/P was closer to the predictions of thermodynamic modeling. The results indicated that the thermodynamic modeling of $FePO_4{\cdot}2H_2O$ precipitation could be utilized to predict the technology parameters for phosphorus removal and recovery.

1. Introduction

Phosphorus in wastewater is one of the important environmental pollutants related to water eutrophication [1]. People have suffered a great deal from pollution by wastewater containing phosphorus. Moreover, phosphorus is one of the most understood non-renewable available nutrients for fertilizer production [2]. Phosphorus reserves will be depleted in recent 60–130 years [3]. As a consequence, phosphorus removal and recovery from wastewater has been considered as an important environmental sustainability concern [4].

Chemical precipitation with iron, alum, lime, and magnesium are the main common treatments for phosphorus removal from wastewater [5–8]. Magnesium ammonium phosphate is used in a potentially effective way to recover phosphorus in a form that can be used as commercial fertilizer. However, widespread application of this method is limited by the high cost of magnesium and the requirement of high pH (>8.5) [9,10]. The application of calcium–phosphorus precipitation is limited by the negatively affect of calcium carbonates precipitation. Carbonate is competing with phosphate for calcium, especially at pH 9.0–11.0, creating a precipitate with relative low phosphorus content [11,12]. Aluminum salts are not practical to use as fertilizer considering the public health concerns of aluminum, thus no attention has been paid to the reuse of the removed phosphorus [13]. Compared with alum, iron salts are more promising in the practical application of phosphorus removal and recovery because of their relatively low cost and high phosphorus removal efficiency [14]. Zhou et al. [14] selected ferric chloride as a coagulant and tannic acid as a coagulant aid to remove phosphorus from different kinds of wastewater. The total-P removal ratios of 94%, 93%, and 96% were achieved for artificial sewage, sewage from wastewater treatment plant, and pesticide industrial wastewater, respectively. Seida and Nakano [15] successfully removed more than 80% of the phosphate from wastewater using the iron-based layered double hydroxides. Ivanov et al. [16] studied the process of phosphate removal from reject water using the reduction of iron ore by the iron-reducing bacteria and obtained a phosphorus removal efficiency of about 90%. De Haas et al. [17] focused on the simultaneous chemical precipitation (iron) of phosphate in the biological excess P removal (BEPR) systems. Many former studies on phosphorus wastewater treatment were tested with ferric precipitation and obtained some empirical parameters. However, a lot of factors, such as pH, Fe^{3+} and PO_4^{3-} concentration, alkalinity, ionic strength, and temperature

* Corresponding author. Tel.: +86 25 83596781; fax: +86 25 83707304.
E-mail address: hqren@nju.edu.cn (H. Ren).

0304-3894/$ – see front matter © 2009 Elsevier B.V. All rights reserved.
doi:10.1016/j.jhazmat.2009.11.049

Table 1
Chemical composition of feed solution and microelement.

Chemical composition of feed solution (mg/L)		Chemical composition of microelement (μg/L)	
$C_6H_{12}O_6$	2500	$FeCl_3{\cdot}4H_2O$	80
NH_4Cl	500	$CoCl_2{\cdot}6H_2O$	80
KH_2PO_4	100	$MnCl_2{\cdot}4H_2O$	20
$NaHCO_3$	132	$(NH_4)_6Mo_7O_2$	4
$CaCl_2$	8	$NiCl_2{\cdot}6H_2O$	2
$MgSO_4$	8	$CuCl_2{\cdot}2H_2O$	1.2

that influence phosphorus precipitation from different conditions of local wastewater, hamper the wide application of iron salts. In order to solve the problem, some studies presented theoretical models for phosphorus removal by ferric iron salts. Fytianos et al. [18] developed a chemical precipitation mathematical model and tested the model with available experimental data of phosphorus removal by ferric iron salts. Takacs et al. [19] performed titration experiments and mathematical modeling to develop the role of ferric phosphate precipitation in phosphorus removal.

The mathematical modeling calculation used to evaluate the effect of solution factors on ferric phosphate ($FePO_4{\cdot}2H_2O$) precipitation, while effective, may be very complicated and time consuming. PHREEQC program (version 2.15) [20], a low-temperature aqueous geochemical calculations computer program, can be applied in saturation-index (SI) calculations and speciation analysis for modeling precipitation–dissolution chemical equilibrium. The thermodynamic modeling calculation with the PHREEQC program may develop a theoretical guide for the effect of reaction conditions on chemical precipitation and optimum technology parameters for phosphorus removal and recovery. Chemical precipitation thermodynamic modeling of the PHREEQC program for calcium phosphate [21] and magnesium ammonium phosphate (MAP) [22] has been investigated in previous studies.

The basic chemical reaction to form $FePO_4{\cdot}2H_2O$ has been expressed in Eq. (1) [20,23]:

$$Fe^{3+} + PO_4^{3-} + 2H_2O \rightarrow FePO_4{\cdot}2H_2O \downarrow \quad (1)$$

In this paper, thermodynamic modeling of the PHREEQC program for phosphorus removal and recovery by $FePO_4{\cdot}2H_2O$ precipitation was undertaken. The factors of $FePO_4{\cdot}2H_2O$ precipitation including pH, Fe^{3+}:PO_4^{3-} molar ratio (Fe/P), initial PO_4^{3-} concentration, alkalinity, ionic strength, and temperature were studied. In order to provide comparison, with the evaluation of thermodynamic modeling as basis, the case study of phosphate removal from anaerobic supernatant was undertaken. Furthermore, surface characterization of $FePO_4{\cdot}2H_2O$ precipitation was analyzed.

2. Materials and methods

2.1. PHREEQC program modeling theory

Gibbs free energy (ΔG), the thermodynamic driving force of a chemical reaction, is the criterion to use in judging whether a reaction is spontaneous ($\Delta G < 0$), in equilibrium ($\Delta G = 0$), or impossible ($\Delta G > 0$) [24]. Gibbs free energy is given in Eq. (2)

$$\Delta G = -\frac{RT}{n} \ln \frac{IAP}{K_{SP}} \quad (2)$$

where R is the ideal gas constant, T is the absolute temperature, n is the number of ions in a formula unit, IAP is the free ionic activities product and K_{SP} is the thermodynamic solubility product.

Supersaturation is the thermodynamic measure for the crystallization of a dissolved salt [25,26]. SI is used to judge the supersaturation of a precipitate phase in a solution and defined as [20]

$$SI = \log \frac{IAP}{K_{SP}} \quad (3)$$

The relationship between ΔG and SI has been expressed in Eq. (4):

$$\Delta G = -\frac{2.303RT}{n} SI \quad (4)$$

SI can be selected as an indicator to measure the thermodynamic basis for the crystallization reaction. The solution is in equilibrium (SI = 0, $\Delta G = 0$), undersaturated (SI < 0, $\Delta G > 0$), or supersaturated (SI > 0, $\Delta G < 0$) [21,22]. The variation of SI and speciation with different solution conditions can be evaluated by the PHREEQC program (version 2.15). The thermodynamic solubility product of $FePO_4{\cdot}2H_2O$ reported by Smith and Martel [23], $\log K_{SP} = -26.40$ (25 °C) is adopted. Therefore, the thermodynamic modeling of $FePO_4{\cdot}2H_2O$ precipitation–dissolution chemical equilibrium can be investigated by the PHREEQC program.

2.2. Raw wastewater

Phosphate wastewater used in the case study was collected from laboratory scale static anaerobic cultivation experiments (batch experiments). Anaerobic granular sludge was obtained from an aeration tank of civil sewage treatment plant near Nanjing. The washed anaerobic granular sludge (300 mL), feed solution (200 mL), and microelement (3–4 drops) were added to a serum bottle (airproofed by rubber plug), cultivated at a temperature of 35 °C, pH of 6.5–7.5, and hydraulic retention time of 24 h (i.e. every 24 h, the steps of pouring out 100 mL anaerobic supernatant from the serum bottle and adding 100 mL feed solution and 3–4 drops microelement into the serum bottle were performed). Table 1 shows the chemical composition of feed solution and microelement. The quality of anaerobic granular sludge and the characteristics of anaerobic supernatant were steady when the static anaerobic cultivation experiments were performed for 3–4 weeks. Then, the anaerobic supernatant was taken out and filtered for experimental used. Table 2 shows the characteristics of anaerobic supernatant.

2.3. Experimental procedures

Modeling for $FePO_4{\cdot}2H_2O$ precipitation were performed as follows. The solution conditions of pH (1–10), PO_4^{3-} (5–300 mg/L), Fe/P (0.1–3.0), alkalinity (5–500 mmol/L), KNO_3 (5–500 mmol/L, taken as electrolyte to adjust the solution ionic strength), and

Table 2
Characteristics of anaerobic supernatant.

Parameter	Unit	Range
COD	mg/L	350 ± 30
NH_4^+-N	mg/L	130 ± 10
PO_4^{3-}-P	mg/L	20 ± 5
Alkalinity ($CaCO_3$)	mg/L	200 ± 20
pH	–	6.5–7.5
Temperature	°C	25–35

Table 3
Calculation equations of thermodynamic modeling between SI and pH.

P concentration (mg/L)	R^2	Calculation equations
20	0.9955	$SI = -4.0137 + 3.7904 \times pH + -0.3458 \times pH^2$
50	0.9927	$SI = -3.8818 + 3.9399 \times pH + -0.3542 \times pH^2$
200	0.9854	$SI = -3.7420 + 4.1564 \times pH + -0.3654 \times pH^2$

temperature (0–35 °C) were designed and inputted. The compiled programs were calculated with the WATEQ4F database. The SI and ion speciation of the crystallization system of $FePO_4{\cdot}2H_2O$ were obtained in the output files and used as basis to formulate the relation models between the SI and the solution conditions. Then, the effects of the solution conditions on $FePO_4{\cdot}2H_2O$ precipitation were evaluated.

Experiments for phosphate removal were performed as follows. Firstly, ferric chloride ($FeCl_3{\cdot}6H_2O$) was added to the wastewater samples. Secondly, the reaction solution was agitated 5 min (200 rpm) for coagulation and 15 min (60 rpm) for flocculation while the pH was regulated at a given experimental level (1.0–10.0) during the process. Thirdly, the formed precipitate was allowed to settle in the reaction solution for 30 min. Lastly, the reaction solution was filtered through a 0.45 μm membrane filter. The precipitate was collected for surface characterization analysis and the supernatant was collected to measure PO_4^{3-} concentration.

2.4. Analytical methods

The concentration of PO_4^{3-} was measured according to the Standard Methods [27]. The collected precipitate was washed with deionized water, and then centrifugally separated. The process was repeated 3 times. The washed precipitate was dried in an oven at 25 °C for 48 h, and then analyzed by a scanning electron microscope analysis (SEM, S-3400N, Hitachi, Japan), X-ray diffraction (XRD, X/TRA, ARL, Switzerland), Fourier transform infrared spectroscopy (FTIR, NEXUS870, USA).

3. Results and discussion

3.1. pH modeling

The modeling was used to evaluate the effect of pH on the SI and the ion species of $FePO_4{\cdot}2H_2O$ precipitation. The pH modeling range was 1.0–10.0. Fig. 1a showed that the SI of $FePO_4{\cdot}2H_2O$ followed a polynomial function of pH (Table 3), and the maximum SI range for $FePO_4{\cdot}2H_2O$ precipitation was observed at the pH of 5.0–6.0. An increase in pH from 1.0 to 5.5 caused a significant increase in SI. With an increase in pH from 5.5 to 10.0, the SI gradually decreased. The lower the pH, the more difficult it is for Fe^{3+} to release H^+ from $H_2PO_4^-$. The higher the pH, the stronger the OH^- compete with PO_4^{3-} for Fe^{3+} [28]. In addition, the pH effect on $FePO_4{\cdot}2H_2O$ precipitation could also be explained by its influence on the speciation of phosphate and ferric iron salts. Under the modeling solution conditions, 9 ferric iron salts species (i.e. Fe^{3+}, $Fe(OH)_2^+$, $Fe(OH)_3$, $FeOH^{2+}$, $Fe(OH)_4^-$, $FeH_2PO_4^{2+}$, $FeHPO_4^+$, $Fe_2(OH)_2^{4+}$, $Fe_3(OH)_4^{5+}$) and 6 phosphate species (i.e. $FeH_2PO_4^{2+}$, $FeHPO_4^+$, $H_2PO_4^-$, HPO_4^{2-}, $KHPO_4^-$, PO_4^{3-}) were formed. The speciation variations of phosphate at different pH (Fig. 1b) showed that with an increase in pH, the ion activities of PO_4^{3-}, HPO_4^{2-}, $KHPO_4^-$ increased; the ion activities of $FeH_2PO_4^{2+}$, $FeHPO_4^+$ decreased; and the ion activity of $H_2PO_4^-$ exhibited no obvious changes. An increase in pH resulted in the dissociation of the species of $FeH_2PO_4^{2+}$, $FeHPO_4^+$ and the association of the species of PO_4^{3-}, HPO_4^{2-}, $KHPO_4^-$. The solution pH could influence the ion activities of ferric iron salts and phosphate, and further change the SI of $FePO_4{\cdot}2H_2O$. Therefore, the solution pH was an effective factor for $FePO_4{\cdot}2H_2O$ precipitation.

There are some relevant papers dealing with the effect of pH on phosphate removal. Fytianos et al. [18] obtained the optimum phosphate removal ratio at a pH of 4.5 and a Fe/P molar ratio of 1:1. Szabo et al. [29] conducted batch and continuous experiments using ferric iron salts to remove phosphate and obtained the best orthophosphate removal efficiency at a pH range of 5.0–7.0. These results are in similar range as our modeling results.

3.2. Fe/P and initial PO_4^{3-} concentration modeling

It has been noted in previous studies that the phosphate removal efficiency was generally affected by the factors of Fe/P and initial PO_4^{3-} concentration [18,19]. The modeling investigated the effect of Fe/P and initial PO_4^{3-} concentration on $FePO_4{\cdot}2H_2O$ precipitation. Fig. 2a was the relationship between SI and Fe/P. The Fe/P modeling range was 0.1–3.0. The SI of $FePO_4{\cdot}2H_2O$ obviously increased with an increase in Fe/P and followed a logarithmic function of Fe/P (Table 4). Fig. 2b showed the effect of the initial PO_4^{3-} concentration on the SI of $FePO_4{\cdot}2H_2O$. The initial PO_4^{3-} concentration modeling range was 5–300 mg/L. The SI value increased significantly with an increase in initial PO_4^{3-} concentration and

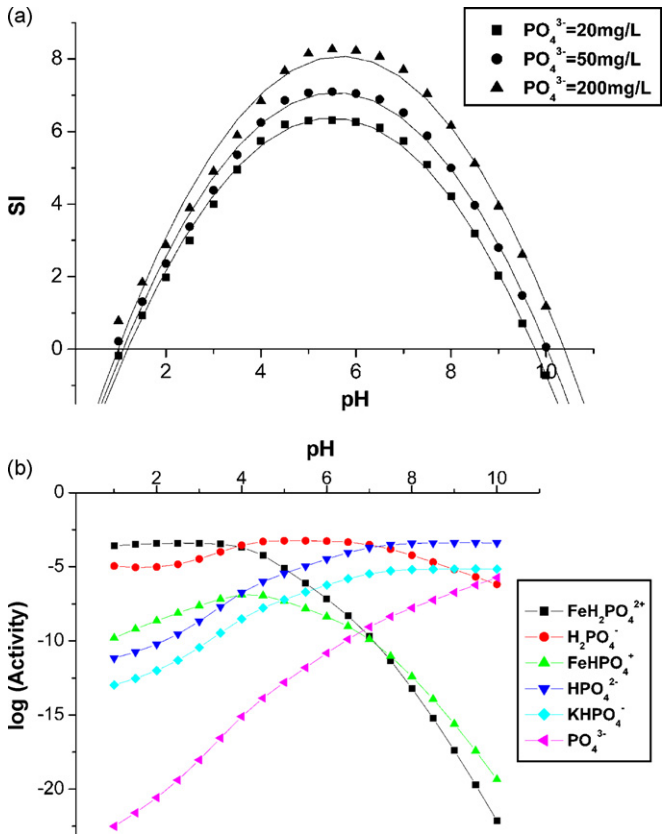

Fig. 1. The effect of pH on $FePO_4{\cdot}2H_2O$ precipitation. (a) SI calculation of $FePO_4{\cdot}2H_2O$ at different pH (Fe^{3+}:PO_4^{3-} = 2:1, temperature = 25 °C, KNO_3 = 10 mmol/L); (b) ion activity at different pH (PO_4^{3-} = 20 mg/L, Fe^{3+}:PO_4^{3-} = 2:1, temperature = 25 °C, KNO_3 = 10 mmol/L).

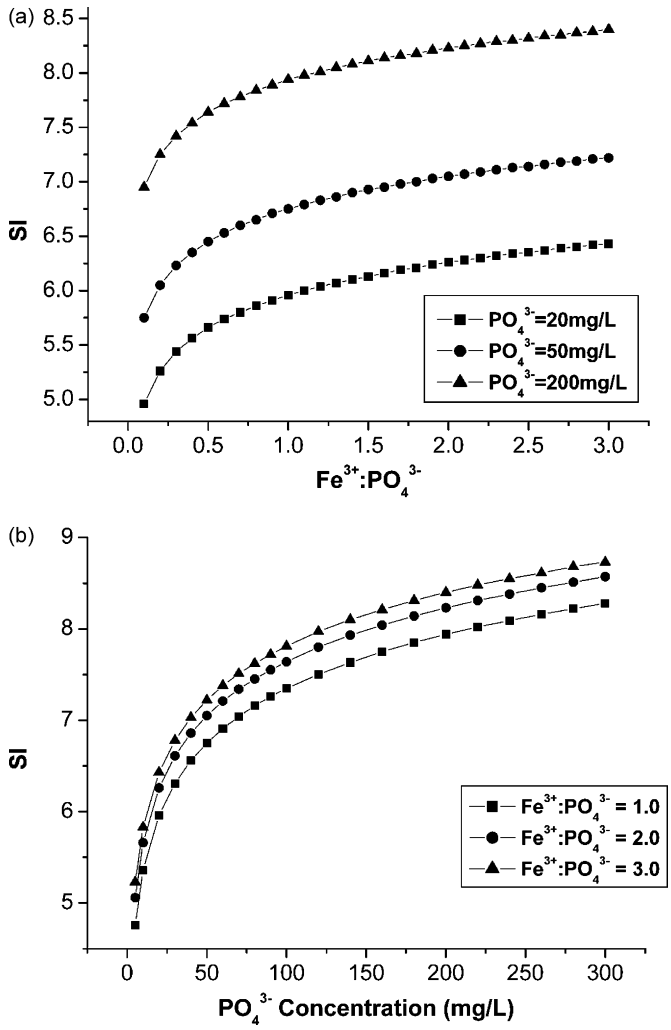

Fig. 2. The effect of Fe/P and initial PO_4^{3-} concentration on $FePO_4{\cdot}2H_2O$ precipitation. (a) SI calculation of $FePO_4{\cdot}2H_2O$ at different Fe^{3+}:PO_4^{3-} molar ratio (pH 6.0, temperature = 25 °C, KNO_3 = 10 mmol/L). (b) SI calculation of $FePO_4{\cdot}2H_2O$ at different initial PO_4^{3-} concentration (pH 6.0, temperature = 25 °C, KNO_3 = 10 mmol/L).

Table 4
Calculation equations of thermodynamic modeling between SI and Fe^{3+}:PO_4^{3-} molar ratio.

P concentration (mg/L)	R^2	Calculation equations
20	1	SI = 0.4328 × ln(Fe/P) + 5.9578
50	0.9999	SI = 0.4325 × ln(Fe/P) + 6.7492
200	0.9999	SI = 0.4252 × ln(Fe/P) + 7.9339

also followed a logarithmic function of initial PO_4^{3-} concentration (Table 5). The results indicated the phosphate removal ratio increased with an increase in Fe/P and initial PO_4^{3-} concentration, respectively.

The SI of $FePO_4{\cdot}2H_2O$ could be calculated and the feasibility of $FePO_4{\cdot}2H_2O$ precipitation could be evaluated under the modeling solution conditions. The reason of Fe/P and initial PO_4^{3-} concentration effect on the SI of $FePO_4{\cdot}2H_2O$ could be explained as Eq. (5):

$$\mathrm{SI} = \log \frac{\mathrm{IAP}}{K_{\mathrm{SP}}} = \log[(C_{\mathrm{Fe^{3+}}} f_1)(C_{\mathrm{PO_4^{3-}}} f_2)] - \log K_{\mathrm{SP}} \quad (5)$$

where $C_{Fe^{3+}}$, $C_{PO_4^{3-}}$ are the concentrations of Fe^{3+}, PO_4^{3-} and f_1, f_2 are the ionic activity coefficient. The Eq. (5) demonstrated the SI of $FePO_4{\cdot}2H_2O$ was correlated with the concentrations of Fe^{3+}, PO_4^{3-} and the coefficient of ionic activity. When the modeling solution conditions, i.e. one of the two ions concentrations (Fe^{3+}, PO_4^{3-}) and the ionic strength were determined, the SI of $FePO_4{\cdot}2H_2O$ followed the logarithmic function of the concentration of the other of the two ions (Fe^{3+}, PO_4^{3-}). As a result, the control of Fe/P and initial PO_4^{3-} concentration was effective for $FePO_4{\cdot}2H_2O$ precipitation.

In the literature, Song et al. [21] studied the effects of solution conditions on hydroxyapatite precipitation and demonstrated the SI was the logarithmic function of phosphate and calcium concentrations, respectively. Wang et al. [22] modeled the crystallization of MAP and indicated the SI value was followed a logarithmic function of the reaction ions concentrations.

Table 5
Calculation equations of thermodynamic modeling between SI and initial PO_4^{3-} concentration.

Fe^{3+}:PO_4^{3-}	R^2	Calculation equations
1.0	1	SI = 0.8594 × ln(PO_4^{3-} concentration) + 3.3859
2.0	1	SI = 0.8561 × ln(PO_4^{3-} concentration) + 3.6951
3.0	0.9999	SI = 0.8551 × ln(PO_4^{3-} concentration) + 3.8684

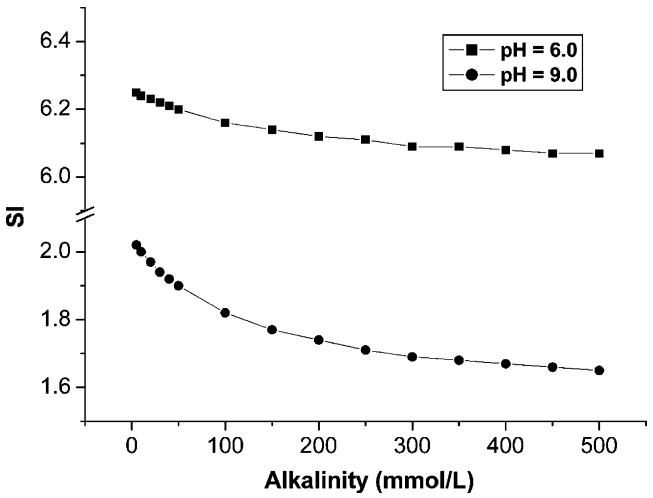

Fig. 3. SI calculation of $FePO_4{\cdot}2H_2O$ at different alkalinity (PO_4^{3-} = 20 mg/L, Fe^{3+}:PO_4^{3-} = 2:1, temperature = 25 °C, KNO_3 = 10 mmol/L).

3.3. Alkalinity modeling

The modeling was formulated to study the effect of alkalinity on $FePO_4{\cdot}2H_2O$ precipitation. The alkalinity modeling range was 5–500 mmol/L. Fig. 3 showed that the SI of $FePO_4{\cdot}2H_2O$ decreased with an increase in the solution alkalinity and followed a logarithmic function of alkalinity (Table 6). The SI value decreased greatly at pH 9.0 and not so obviously at pH 6.0. The results demonstrated that alkalinity could decrease the precipitation efficiency of $FePO_4{\cdot}2H_2O$. The formation of ion pairs between alkaline ions (carbonate, bicarbonate, etc.) and ferric ions as well as the decrease of free ferric ions, accounted for this observation. This caused a decrease in the thermodynamic driving force for $FePO_4{\cdot}2H_2O$ precipitation. In practical wastewater treatment, the solution condition of actual alkalinity might be more complicated than that of the modeling alkalinity. Actual alkalinity was defined as all of the ions that could react with proton. The modeling alkalinity was

Table 6
Calculation equations of thermodynamic modeling between SI and alkalinity.

pH	R^2	Calculation equations
6.0	0.9531	SI = −0.0443 × ln(alkalinity) + 6.3535
9.0	0.9712	SI = −0.0905 × ln(alkalinity) + 2.2211

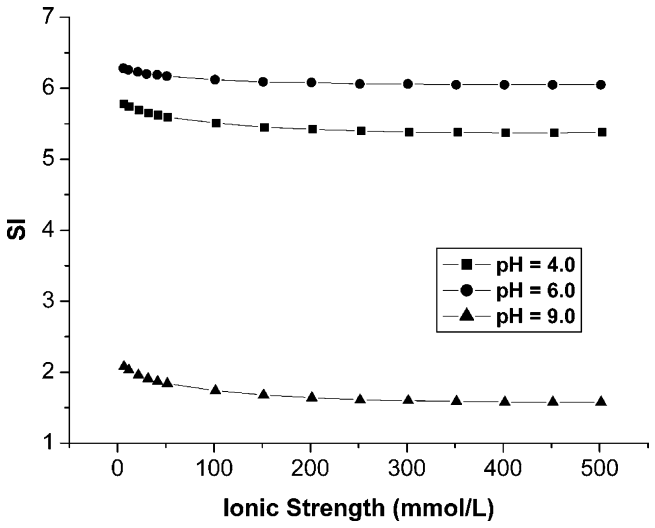

Fig. 4. SI calculation of $FePO_4{\cdot}2H_2O$ at different ionic strength (PO_4^{3-} = 20 mg/L, Fe^{3+}:PO_4^{3-} = 2:1, temperature = 25 °C).

Table 7
Calculation equations of thermodynamic modeling between SI and ionic strength.

pH	R^2	Calculation equations
4.0	0.9873	SI = −0.105 × ln(ionic strength) + 5.9986
6.0	0.9869	SI = −0.0581 × ln(ionic strength) + 6.3949
9.0	0.9913	SI = −0.1262 × ln(ionic strength) + 2.3324

assumed to be that of carbonate to simplify the model. Thus, the factor of solution alkalinity might be more important in the practical phosphate wastewater treatment by $FePO_4{\cdot}2H_2O$ precipitation. Szabo et al. [29] conducted research on the effect of alkalinity on ferric addition in wastewater treatment for phosphorus removal and considered alkalinity as a key factor for $FePO_4{\cdot}2H_2O$ precipitation.

3.4. Ionic strength modeling

The effect of ionic strength on $FePO_4{\cdot}2H_2O$ precipitation was investigated (Fig. 4). The KNO_3 modeling range was 5–500 mmol/L. With the solution ionic strength increasing, the SI of $FePO_4{\cdot}2H_2O$ decreased and followed a logarithmic function of ionic strength (Table 7). An increase in the ionic strength caused a decrease in $FePO_4{\cdot}2H_2O$ precipitation. Eq. (5) demonstrated the concentrations of ferric iron salts and phosphate as well as the coefficient of ionic activity influenced the SI of $FePO_4{\cdot}2H_2O$. When the modeling concentrations of Fe^{3+}, PO_4^{3-} were determined, the SI of $FePO_4{\cdot}2H_2O$ followed the logarithmic function of ionic strength. In practical wastewater treatment, the ionic strength was influenced by the different local water conditions. Donnert [30] reported that the wastewater ionic strength was 0.021 M in the Germany hard water area and 0.011 M in the Japanese wastewater. Although the ionic strength was difficult to adjust for the treatment of hard wastewater, the concentrations of wastewater could be diluted at certain conditions under the evaluation of thermodynamic modeling to avoid the influence of ionic strength.

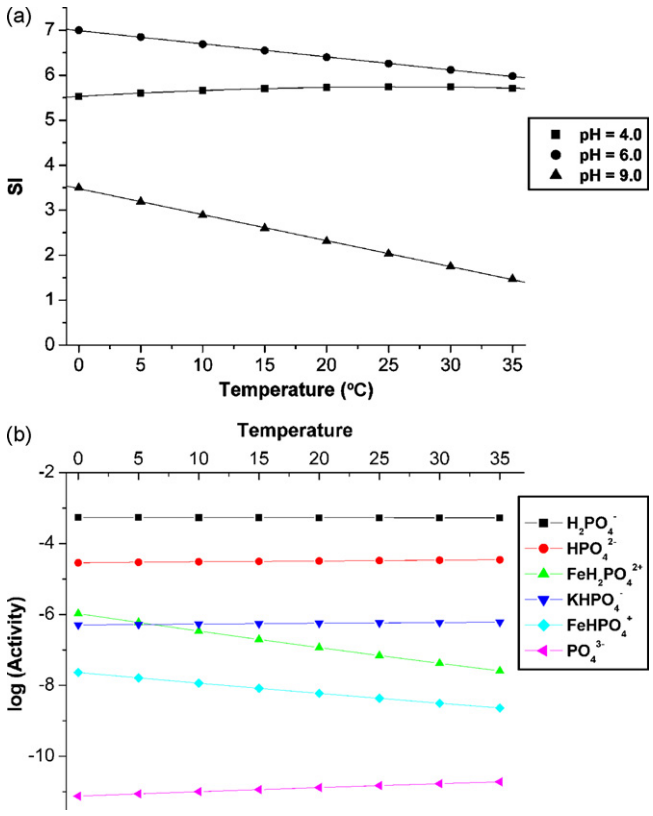

Fig. 5. The effect of temperature on $FePO_4{\cdot}2H_2O$ precipitation. (a) SI calculation of $FePO_4{\cdot}2H_2O$ at different temperature (PO_4^{3-} = 20 mg/L, Fe^{3+}:PO_4^{3-} = 2:1, KNO_3 = 10 mmol/L); (b) ion activity at different temperature (pH 6.0, PO_4^{3-} = 20 mg/L, Fe^{3+}:PO_4^{3-} = 2:1, KNO_3 = 10 mmol/L).

3.5. Temperature modeling

The modeling investigated the effect of temperature on $FePO_4{\cdot}2H_2O$ precipitation. The temperature modeling range was 0–35 °C. Fig. 5a showed that at pH 6.0 and 9.0, the SI value decreased with an increase in temperature and followed a linear function; at pH 4.0, the SI value increased at the early stage and decreased later, and followed a polynomial function (Table 8). At pH 6.0 and 9.0, the yield of $FePO_4{\cdot}2H_2O$ decreased with an increase in temperature from 0 to 35 °C. At pH 4.0, the optimal temperature range for $FePO_4{\cdot}2H_2O$ precipitation was 25–30 °C. The association/dissociation reactions of $FePO_4{\cdot}2H_2O$ could be evaluated by the speciation of phosphate and ferric iron salts at different temperature. Fig. 5b showed that with an increase in temperature, the ion activities of $H_2PO_4^-$, HPO_4^{2-}, $KHPO_4^-$ exhibited no obvious changes, while the ion activities of $FeH_2PO_4^{2+}$, $FeHPO_4^+$ decreased, and the ion activity of PO_4^{3-} increased. An increase in temperature caused the dissociation of the species of $FeH_2PO_4^{2+}$, $FeHPO_4^+$ and the association of the species of PO_4^{3-}. The temperature could influence the ion activity of ferric iron salts and phosphate, and thus change the SI of $FePO_4{\cdot}2H_2O$. In view of these observations, the factor of solution temperature should be considered in the conduct of practical phosphate wastewater treatment by $FePO_4{\cdot}2H_2O$ precipitation.

Table 8
Calculation equations of thermodynamic modeling between SI and temperature.

pH	R^2	Calculation equations
4.0	0.9986	SI = 5.5279 + 0.0164 × temperature − 3.1667 × temperature^2
6.0	0.9971	SI = 6.9908 − 0.0291 × temperature
9.0	0.9996	SI = 3.4792 − 0.0578 × temperature

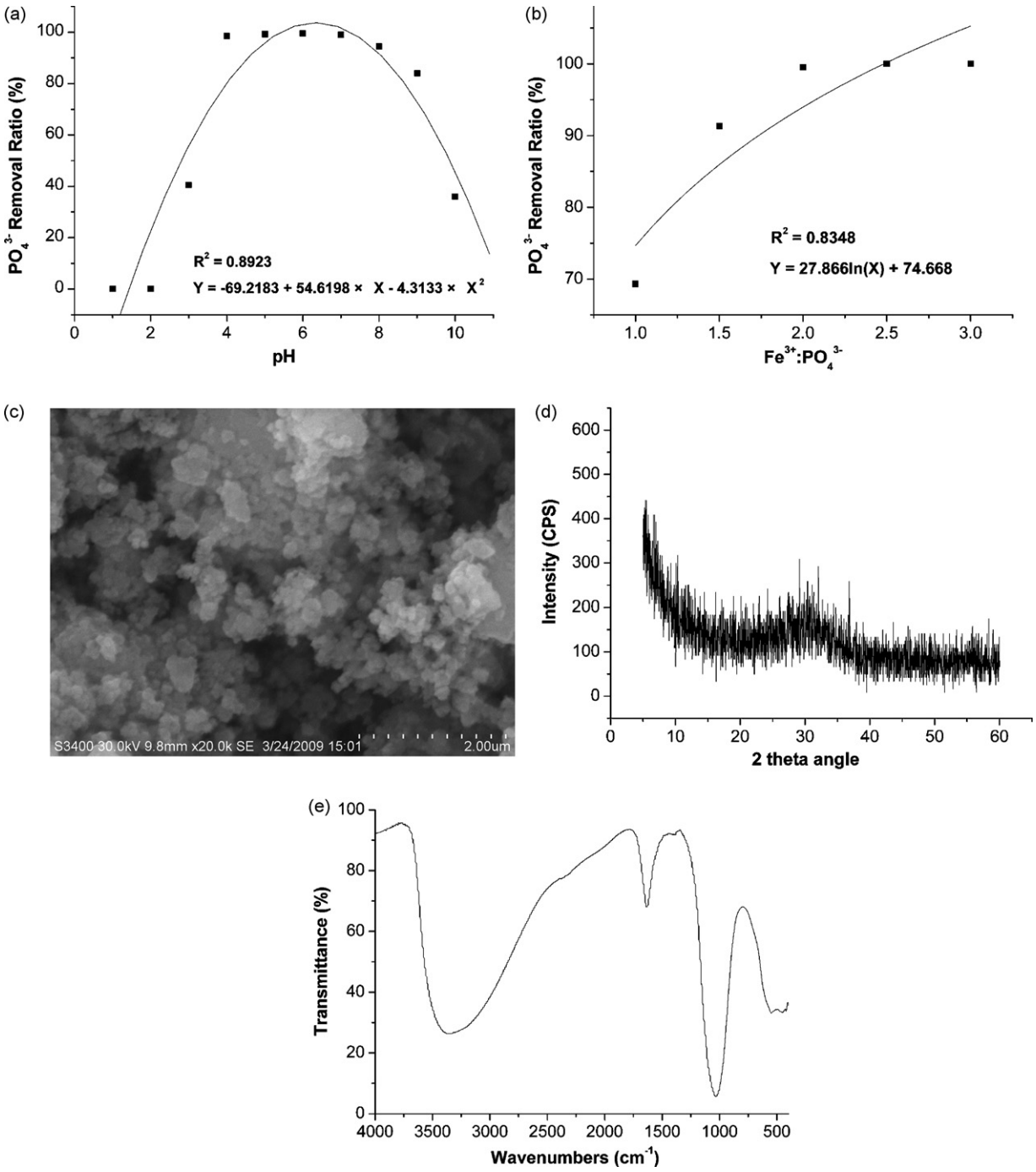

Fig. 6. Phosphate removal from anaerobic supernatant. (a) PO_4^{3-} removal ratio at different pH (Fe^{3+}:PO_4^{3-} = 2:1). (b) PO_4^{3-} removal ratio at different Fe^{3+}:PO_4^{3-} molar ratio (pH 6.0). (c) Scanning electron microscopy analysis of $FePO_4{\cdot}2H_2O$ precipitate. (d) X-ray diffraction analysis of $FePO_4{\cdot}2H_2O$ precipitate. (e) Fourier transform infrared spectroscopy analysis of $FePO_4{\cdot}2H_2O$ precipitate.

3.6. Case study of phosphate removal from anaerobic supernatant

Compared with thermodynamic modeling of $FePO_4{\cdot}2H_2O$ precipitation, the experiments on phosphate removal from anaerobic supernatant by $FePO_4{\cdot}2H_2O$ precipitation was investigated. It was concluded that the experimental results were closer to the predictions of thermodynamic modeling.

Fig. 6a showed the optimum pH range for phosphate removal was 4.0–7.0. The experimental results were in qualitative agreement with the linear correlation of the SI for $FePO_4{\cdot}2H_2O$ precipitation (Fig. 1a). The small deviations in the trend in phosphate removal experiments were responsible for the co-precipitation of $FePO_4{\cdot}2H_2O$ and $Fe(OH)_3$, the adsorption of hydrolyzed ferric iron salts [31], and the flocculation effects [19]. The optimum Fe/P range was 1.5–2.0 (Fig. 6b). When the Fe/P increased from 1:1 to 2:1, the phosphate removal ratio also increased; however, further increase in Fe/P was not economical for additional phosphate removal and recovery. The linear correlation of the experimental data was similar to a logarithmic function and reasonably agreed with the thermodynamic modeling predictions for $FePO_4{\cdot}2H_2O$ precipitation (Fig. 2a). Both modeling and experiments indicated that ferric iron salts was the limiting constituent for $FePO_4{\cdot}2H_2O$ precipitation. In order to maximize the reduction of soluble phosphorus, a ferric iron source was required.

SEM analysis (Fig. 6c) was performed to identify the surface characterization of the precipitate, and it showed that the spherical crystals were unshaped and coarse. XRD analysis (Fig. 6d) indicated that the precipitate was amorphous solid. FTIR pattern (Fig. 6e) showed the infrared spectrum of the precipitate was close to that of $FePO_4{\cdot}2H_2O$ as elucidated elsewhere [31].

The thermodynamic modeling of $FePO_4{\cdot}2H_2O$ precipitation can provide a theoretical guide for operational parameters design and evaluate the effect of solution conditions on phosphate removal, although practical phosphate wastewater treatment is complicated. When modeling data are entered into the PHREEQC program, it is easy to conduct iterative analyses for the various amendments to evaluate the operational parameters. Thermodynamic modeling can develop a useful method to optimize the technology parameters of phosphate removal and recovery for all kinds of wastewater.

4. Conclusions

To study phosphorus removal and recovery from wastewater, a thermodynamic modeling assessment and a case study were investigated. The following conclusions were drawn.

(1) SI was utilized to indicate the thermodynamic modeling for $FePO_4{\cdot}2H_2O$ precipitation. The SI of $FePO_4{\cdot}2H_2O$ followed a polynomial function of pH, and the solution pH influenced the ion activities of ferric iron salts and phosphate. As a result, pH was an important factor for $FePO_4{\cdot}2H_2O$ precipitation.
(2) The SI of $FePO_4{\cdot}2H_2O$ increased, and it followed a logarithmic function of Fe/P and initial PO_4^{3-} concentration, respectively. Therefore, the control of Fe/P and initial PO_4^{3-} concentration was effective for $FePO_4{\cdot}2H_2O$ precipitation.
(3) The SI of $FePO_4{\cdot}2H_2O$ decreased, and it was described by a logarithmic function of alkalinity and ionic strength, respectively. With an increase in temperature, SI at pH 6.0 and 9.0 decreased with a linear function; SI at pH 4.0 followed a polynomial function. The research showed that the factors of alkalinity, ionic strength, and temperature influenced the $FePO_4{\cdot}2H_2O$ precipitation from wastewater.
(4) In the case study of phosphate removal from anaerobic supernatant, the phosphate removal trend at different pH and Fe/P was reasonably closer to the thermodynamic modeling predictions. SEM analysis indicated that the spherical crystals were unshaped and coarse. XRD analysis demonstrated that the precipitate was amorphous solid. FTIR pattern showed that the infrared spectrum of the precipitate was similar to that of $FePO_4{\cdot}2H_2O$. Therefore, chemical precipitation thermodynamic modeling of $FePO_4{\cdot}2H_2O$ precipitation can provide a theoretical guide for technology parameters design and evaluate the effect of solution conditions on phosphorus removal and recovery.

Acknowledgements

The authors are indebted the anonymous reviewers for their insightful comments and suggestions that significantly improved the manuscript. The work was supported by a grant from the Social Development Foundation of Jiangsu Province (No. BS2008006), the Science and Technology Key Research Projects of Ministry of Education of the People's Republic of China (No. 108150), and the Scientific Research Foundation of Graduate School of Jiangsu Province (No. CX09B_013Z). Thanks to the Modern Analysis Center of Nanjing University.

References

[1] L.R. Cooperband, L.W. Good, Biogenic phosphate minerals in manure: implications for phosphorus loss to surface waters, Environ. Sci. Technol. 36 (23) (2002) 5075–5082.
[2] A. Montangero, H. Belevi, Assessing nutrient flows in septic tanks by eliciting expert judgment: a promising method in the context of developing countries, Water Res. 41 (2007) 1052–1064.
[3] I. Steen, Phosphorus availability in the 21st century: management of a non-renewable resource, Phosphorus Potassium 217 (1998) 25–31.
[4] G.K. Morse, S.W. Brett, J.A. Guy, J.N. Lester, Review: phosphorus removal and recovery technologies, Sci. Total Environ. 212 (1998) 69–81.
[5] L.E. de-Bashan, Y. Bashan, Recent advances in removing phosphorus from wastewater and its future use as fertilizer (1997–2003), Water Res. 38 (2004) 4222–4246.
[6] Y. Wang, T. Han, Z. Xu, G. Bao, T. Zhu, Optimization of phosphorus removal from secondary effluent using simplex method in Tianjing, China, J. Hazard. Mater. B121 (2005) 183–186.
[7] E. Kim, S. Yim, H. Jung, E. Lee, Hydroxyapatite crystallization from a highly concentrated phosphate solution using powdered converter slag as a seed material, J. Hazard. Mater. B136 (2006) 690–697.
[8] J.A. Wilsenach, C.A.H. Schuurbiers, M.C.M. van Loosdrecht, Phosphate and potassium recovery from source separated urine through struvite precipitation, Water Res. 41 (2007) 458–466.
[9] J.D. Doyle, S.A. Parsons, Struvite formation, control and recovery, Water Res. 36 (2002) 3925–3940.
[10] T. Zhang, L. Ding, H. Ren, Pretreatment of ammonium removal from landfill leachate by chemical precipitation, J. Hazard. Mater. 166 (2009) 911–915.
[11] L. Montastruc, C. Azzaro-Pantel, B. Biscans, M. Cabassud, S. Domenech, A thermochemical approach for calcium phosphate precipitation modeling in a pellet reactor, Chem. Eng. J. 94 (2003) 41–50.
[12] Y. Song, H.H. Hahn, E. Hoffmann, The effect of carbonate on the precipitation of calcium phosphate, Environ. Technol. 23 (2002) 207–215.
[13] A. Adin, Y. Soffer, R. Ben Aim, Effluent pretreatment by iron coagulation applying various dose-pH combinations for optimum particle separation, Water Sci. Technol. 38 (6) (1998) 27–34.
[14] Y. Zhou, X. Xing, Z. Liu, L. Cui, A. Yu, Q. Feng, H. Yang, Enhanced coagulation of ferric chloride aided by tannic acid for phosphorus removal from wastewater, Chemosphere 72 (2008) 290–298.
[15] Y. Seida, Y. Nakano, Removal of phosphate by layered double hydroxides containing iron, Water Res. 36 (2002) 1306–1312.
[16] V. Ivanov, S. Kuang, V. Stabnikov, C. Guo, The removal of phosphorus from reject water in a municipal wastewater treatment plant using iron ore, J. Chem. Technol. Biotechnol. 84 (2009) 78–82.
[17] D.W. de Haas, M.C. Wentzel, G.A. Ekama, The use of simultaneous chemical precipitation in modified activated sludge systems exhibiting biological excess phosphate removal Part 1: literature review, Water SA 26 (4) (2000) 439–452.
[18] K. Fytianos, E. Voudrias, N. Raikos, Modelling of phosphorus removal from aqueous and wastewater samples using ferric iron, Environ. Pollut. 101 (1998) 123–130.
[19] I. Takacs, S. Murthy, S. Smith, M. Mcgrath, Chemical phosphorus removal to extremely low levels: experience of two plants in the Washington, DC area, Water Sci. Technol. 53 (12) (2006) 21–28.
[20] D.L. Parkhurst, C.A.J. Appelo, User's Guide to PHREEQC (Version 2)—a computer program for speciation, batch-reaction, one-dimensional transport, and inverse geochemical calculations, Water-Resources Investigations Report 99-4259, US Department of the Interior, US Geological Survey, Denver, Colorado, 1999.
[21] Y. Song, H.H. Hahn, E. Hoffmann, Effects of solution conditions on the precipitation of phosphate for recovery a thermodynamic evaluation, Chemosphere 48 (2002) 1029–1034.
[22] J. Wang, Y. Song, P. Yuan, J. Peng, M. Fan, Modeling the crystallization of magnesium ammonium phosphate for phosphorus recovery, Chemosphere 65 (2006) 1182–1187.
[23] R.M. Smith, A.E. Martel, Critical Stability Constants, vol. 3, Plenum, New York, 1976.
[24] Y. Marcus, Thermodynamics of solvation of ions. 5. Gibbs free energy of hydration at 298.15 K, J. Chem. Soc.-Faraday Trans. 87 (1991) 2995–2999.
[25] W. Stumm, J.J. Morgan, Aquatic Chemistry, third ed., John Wiley and Sons, Inc., New York, 1996, p. 356.
[26] I. Joko, Phosphorus removal from wastewater by the crystallization method, Water Sci. Technol. 17 (1984) 121–132.
[27] APHE, Standard Methods for the Examination of Water and Wastewater, American Public Health Association, Washington, DC, 1998.
[28] P.H. Hsu, Comparison of iron (III) and aluminum in precipitation of phosphate from solution, Water Res. 10 (1976) 903–907.
[29] A. Szabo, I. Takacs, S. Murthy, G.T. Daigger, I. Licsko, S. Smith, Significance of design and operational variables in chemical phosphorus removal, Water Environ. Res. 80 (2008) 407–416.
[30] D. Donnert, Investigations on phosphorus removal from waste water, Progress Report KFK 4459, Kernforschungszentrum Karlsruhe, 1988.
[31] E. Pierri, D. Tsamouras, E. Dalas, Ferric phosphate precipitation in aqueous media, J. Cryst. Growth 213 (2000) 93–98.